The Light Energy Dependence of the *Limulus* Photoreceptor Current in Two Defined States of Adaptation

H. Stieve and B. Schlösser

Institut für Biologie II der RWTH, D-5100 Aachen, Bundesrepublik Deutschland

Z. Naturforsch. **44c**, 999–1014 (1989); received July 10, 1989

Limulus Ventral Nerve Photoreceptor, Light-Induced Receptor Current, Light and Dark Adaptation, Stimulus Response Characteristics, Energy Dependence

The light energy dependence of the *Limulus* ventral nerve photoreceptor current was determined for two reproducible states of adaptation.

In the double logarithmic plot the energy dependence of the current amplitude and that of the current-time integral, which represents the total charge transport through the membrane during the response, show several sections with different slopes:
1) a linear section (slope about 1)
2) a supralinear section (slope 2–4)
3) a sublinear section (slope < 0.5) and
4) a second sublinear section (slope > 0.5, only in current-time integral curve).

A significant deviation from slope 1 indicates that the single events (bumps) which constitute the macroscopic receptor current, are not independent of each other in size and/or number. It may indicate a positive or negative cooperativity.

Light adaptation reduces the size of the receptor current and shifts the response *vs.* energy characteristics towards higher light energies. For light- and dark-adapted cells the transitions between the sections occur at same amplitude or area values, only the light energy values are different.

The energy dependence of the time parameters, which characterize the shape of the light response, shows the same partition in 4 sections as the receptor current. The time parameters are shortened whith increasing stimulus energy and light adaptation. The amount of the shortening is greater in the supralinear section of the amplitude or area *vs.* energy characteristics than in the other sections (except for latency and time-to-peak with greatest shortening in the linear or first sublinear section). Section 4 is correlated with a new increase of response duration and simultaneously with the appearance of the second response component.

The results can be interpreted sufficiently in terms of the bump-speck-model and of an automatic gain control mechanism.

Abbreviations: ReC, receptor current (membrane current signal in response to light stimulus; J_{Max} [nA], peak amplitude of ReC; T_{Lat} [ms], latent-period (time from stimulus begin until first measurable increase of response; T_1 [ms], rise-time (from half to response maximum); T_{Max} [ms], time-to-peak (from stimulus begin); T_2 [ms], decrease-time (from response maximum to half); T_B [ms], response duration; J_M [nA], membrane current; J_D [nA], membrane current in dark during voltage clamp; J_L [nA], amplitude of light-induced current; F [nAs], current-time integral of the light-induced membrane current; LA, (moderate) light adaptation; DA, (considerable) dark adaptation; t_{da} [ms] dark adaptation time; t_α, t_β [ms], delay times between beginning of the conditioning 2 s illumination and test flashes evoking responses in a state of moderate light adaptation (α) and considerable dark adaptation (β); C_1, C_2 conditioning illumination 1 and 2; I_0, maximal energy of test flashes; s_1 first curve section of current response *vs.* stimulus energy curve in double log plot; s_2, s_3, s_4, sections 2, 3, 4; s_1–s_2, transition between s_1 and s_2 (curve-"heel"); s_2–s_3, transition between s_2 and s_3 (curve-"knee"); s_3–s_4, transition between s_3 and s_4 (curve-"hip"); r_1, r_2, r_3, r_4 [log nA/log I] resp. [log nAs/log I], steepness of s_1, s_2, s_3, s_4; PS, physiological saline.

Reprint requests to Prof. Dr. H. Stieve.

Verlag der Zeitschrift für Naturforschung, D-7400 Tübingen
0341–0382/89/1100–0999 $ 01.30/0

Introduction

Absorption of a photon by rhodopsin in the plasma membrane of the *Limulus* photoreceptor cell initiates a sequence of events leading to the generation of the elementary excitatory response, the bump. The number of bumps evoked by a light stimulus increases linearly with the stimulus energy in the lower energy range where individual bumps can be observed [1, 2]. With stronger light energy, the bumps begin to overlap and to fuse to the macroscopic receptor current signal [3]. The proportionality of the number of the light-evoked bumps to the number of absorbed photons should cause a linear rise of the receptor current with increasing stimulus intensity. Lisman and Brown [4] found a linear dependence of the receptor current amplitude only for low light energies from the threshold (flash which evokes on the average one bump) to about 100 times threshold value. In a medium intensity range the receptor current rises "supralinearly", *i.e.* steeper than proportional, with the stimulus energy [5, 6]. At even

higher light intensities the supralinear section is followed by a sublinear section with a steepness smaller than 1 in a double logarithmic plot [5, 7, 8].

Light adaptation reduces the sensitivity of the photoreceptor; one reason is the diminution of the size of the bumps which constitute the receptor current (adapting bump model [3]). The response *vs.* stimulus characteristics are shifted by light adaptation to higher light intensities [7].

We can manipulate the adaptation state by modifying either the light energy of the (conditioning) light-adapting illumination or the time of dark adaptation [9, 10].

In an earlier publication [7] we showed the receptor current characteristics in dependence of the stimulus energy for the dark- and the light-adapted state.

The main intention of the investigations presented in this paper is to investigate the response *vs.* energy characteristics over the whole available light energy range at two defined states of adaptation, in order to determine steepness and extent of the particular sections of this dependence under physiological conditions, and to describe them quantitatively.

Especially the low intensity range, in which individual bumps are detectable and overlap to the macroscopic receptor current, was studied by variation of the test light energy in small steps and multiple repetition of the measurements.

We studied size and time course, characterized by the time parameters, of the receptor current and its dependence on light energy.

Materials and Methods

The excised *Limulus* ventral nerves (for details of the preparation see Stieve and Bruns [11]) were continuously superfused with physiological saline (PS, temperature 15 °C, flow rate 1 ml/min) during the whole experiment. The photoreceptor cell was impaled by two glass microelectrodes to measure under voltage clamp conditions [12], in order to consider only light-activated ion-channels and not voltage-sensitive channels. The responses were digitized (1/ms sample rate), recorded on tape and evaluated by computer with a time resolution of 1 ms. The minimal response amplitude determinable from the noise was about 60 pA.

We stimulated the photoreceptor cells using illumination from two different light sources: For the conditioning we used a 2 s illumination delivered by a halogen lamp with maximal light energy of about 5.6×10^{15} photons/cm^2 s (540 nm). For the test stimuli we used a camera flash (Metz-Mecablitz) with a power of 9×10^{14} photons/cm^2 (540 nm) at a duration of 1 ms. We attenuated this energy value I_0 by changing the flash duration or by neutral density filters (Schott, $I/I_0 = 0.5$). More details are described elsewhere [9, 13].

Procedure

After impalement by the electrodes we stimulated the cell during a preperiod of 10–15 min in 30 s intervals (light intensity of $I/I_0 = 2^{-5}$) until the response amplitudes and the PMP (prestimulus membrane potential) became constant. Then the cell was clamped to the PMP or to a slightly hyperpolarizing potential. If the responses then remained constant too, the stimulus program was started.

Stimulus program

A flash sequence was used to evoke responses in reproducible states of moderate light adaptation (LA) and considerable dark adaptation (DA) (Fig. 1).

A stimulus cycle (cycle time 4 min) consisted of a 2 s conditioning illumination (C_1) followed by two test flashes of identical energy (α and β). The first test flash (α) was applied after a delay time (t_{da}) of 16 s (after the end of C_1), the second (β) after a t_{da} of 118 sec. The α flash evoked responses in a defined state of moderate light adaptation due to the preceding conditioning illumination. The following β flash evoked responses in a state of considerable dark adaptation. According to Claßen-Linke and Stieve

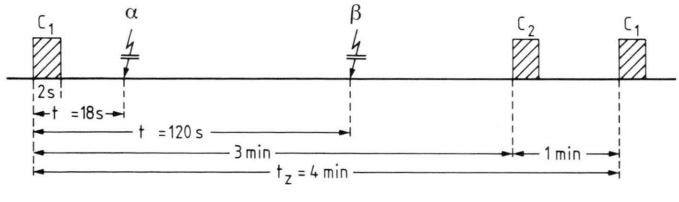

Fig. 1. Stimulus program of one measuring cycle. C_1, C_2: conditioning illumination; α, β: test flashes, duration *ca.* 10 ms, variable energy; t_z: cycle-time.

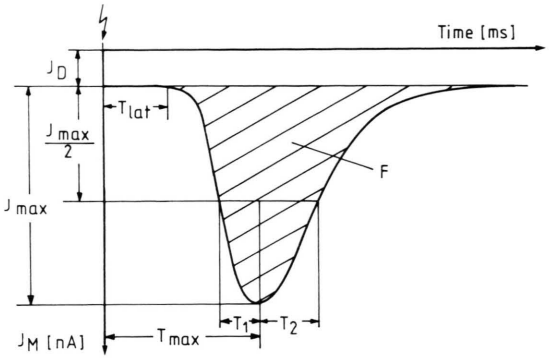

Fig. 2. Explanation of the parameters determined of the receptor current signal (J_M) T_{Lat} (latent-period), T_1 (increase-time), T_{Max} (time-to-peak), T_2 (decrease-time), T_B (duration), J_{Max} (maximal amplitude of current response), F (current-time integral).

[14] about 90% of the dark adaptation in *Limulus* photoreceptors occurs within ca. 2 min.

A second 2 s conditioning stimulus (C_2, identical to C_1) was applied after 3 min in order to abolish an influence of the β response on the effect of the conditioning illumination C_1, which starts the cycle, and so to ensure that the cell was always in the same state of adaptation when C_1 was delivered. The intensity of C_1 and C_2 was adjusted for each experiment in such a way that with a test stimulus energy of $I/I_0 = 2^{-5}$ the current amplitudes evoked by the α flash were about half the current amplitudes evoked by the β flash.

The test flash energy was decreased by filters (factor 2) from cycle to cycle until responses became unmeasurable and then increased again in smaller steps by filters and by changing the flash duration (3 intersteps per filter) up to the maximal available light energy I_0.

In the low intensity range the stimulus sequence was repeated 2 or 3 times with the same stimulus energy. We averaged the response values because of the great scattering of the responses to weak stimulation.

Evaluation

For each receptor current signal the following parameters were determined (Fig. 2):

F (pAs): current-time integral (starting from the end of latency up to the decline of amplitude size to 5% from J_{Max})

J_{Max} (nA): (absolute) maximum of the receptor current signal

T_{Lat} (ms): latency (explanation see below)

T_{Max} (ms): time-to-peak (explanation see below)

T_1 (ms): increase-time from $J_{Max}/2$ to J_{Max}

T_2 (ms): decrease-time from J_{Max} to $J_{Max}/2$

T_B (ms): response duration

If there was more than one individual bump following the light stimulus, we computed the area F from all bumps by addition of the single F values, J_{Max}, however, represents the amplitude maximum of the largest bump. As T_{Max} we defined the duration

Table I. Comparision of steepness and position of sections s_1, s_2, s_3 and s_4 in state of considerable dark adaptation (β) and moderate light adaptation (α), 5 experiments: BS5, BS6, BS7(H4), BS7(H8), BS.8. For response *vs.* energy characteristics of current amplitude J_{Max} and current-time integral F steepness r_1, r_2, r_3 and r_4 [log(I/I_0)/log J] resp. [log(I/I_0)/log F] of the curve sections and transitions s_1-s_2 (heel), s_2-s_3 (knee) and s_3-s_4 (hip) [log(I/I_0)/log J] resp. [log(I/I_0)/log F] are calculated by linear regression.

		BS5		BS6		BS7–H4		BS7–H8		BS 8		averaged values	
current J_{Max}		DA	LA	DA	LA	DA	LA	DA	LA	DA	LA	DA	LA
r_1	[log(I/I_0)/log J]	1.6	1.0	0.7	0.8	1.6	0.9	1.3	1.2	1.0	1.1	1.2±0.17	1.0±0.07
r_2	[log(I/I_0)/log J]	3.5	3.7	3.5	2.0	2.7	2.8	2.7	2.8	3.4	2.8	3.2±0.19	2.8±0.27
r_3	[log(I/I_0)/log J]	(0.56)		0.2	0.2	0.1	0.1	0.1	0.1	0.1	0.2	0.1±0.03	0.2±0.03
r_4	[log(I/I_0)/log J]			0.4	0.6							0.4	0.6
"heel" s_1-s_2	[log(I/I_0)/log J]	−4.0/0.1	−3.2/0.1	−3.7/0.3	−2.4/0.2	−4.1/−0.1	−2.7/−0.1	−4.0/0.5	−3.6/−0.4	−3.5/−0.3	−2.9/0.2	−3.7±0.11/0.3±0.08	−3.0±0.21/0.2±0.05
"knee" s_2-s_3	[log(I/I_0)/log J]	−3.3/2.2		−3.0/2.0	−1.5/2.0	−3.1/2.4	−1.7/2.5	−3.2/2.6	−2.6/2.6	−2.7/2.5	−2.1/2.5	−3.1±0.10/2.3±0.11	−2.0±0.25/2.4±0.14
"hip" s_3-s_4	[log(I/I_0)/log J]			−1.1/2.4	−0.3/2.2							1.1/2.4	0.3/2.2
current-time integral F													
r_1	[log(I/I_0)/log F]	1.9	1.5	1.0	1.0	1.8	1.2	1.7	1.2	1.5	1.1	1.6±0.16	1.2±0.09
r_2	[log(I/I_0)/log F]	2.8	2.6	3.3	1.5	2.7	2.2	2.4	2.3	3.1	2.0	2.7±0.26	1.9±0.37
r_3	[log(I/I_0)/log F]	(0.4)		0.2	0.4	0.2	0.3	0.1	0.1	0.1	0.4	0.2±0.03	0.3±0.07
r_4	[log(I/I_0)/log F]			0.6	0.8					0.4		0.5±0.12	0.8
"heel" s_1-s_2	[log(I/I_0)/log F]	−4.0/2.0	−3.4/2.0	−3.6/2.3	−2.4/2.2	−3.9/2.4	−2.6/2.4	−4.0/2.8	−3.7/1.7	−3.5/2.6	−3.1/2.3	−3.8±0.11/2.4±0.13	−3.0±0.24/2.1±0.13
"knee" s_2-s_3	[log(I/I_0)/log F]	−3.3/3.9		−3.2/3.7	−1.6/3.5	−3.2/4.3	−1.7/4.3	−3.3/4.4	−2.6/4.4	−2.9/4.4	−2.1/4.2	−3.2±0.07/4.1±0.14	−2.0±0.23/4.1±0.25
"hip" s_3-s_4	[log(I/I_0)/log F]			−1.8/4.0	−0.4/4.0					−1.8/4.5		−1.8±0/4.25±0.25	−0.4/4.0

between stimulus begin and J_{Max}, as latency the duration between stimulus begin and first detectable deviation from the baseline.

Because of its similarity to a human leg we describe the shape of the response *vs.* energy characteristics by the respective terms hip, thigh, knee, shank, heel, and foot.

Results

In this work the findings of 5 experiments are compiled, all values – unless stated otherwise – are averaged values ($n=5$), the results are demonstrated for two individual cells in Fig. 3–7 and the evaluation results from the 5 experiments are listed in Table I.

Original registrations of current responses, overlapping of bumps to the macroscopic receptor current

A very weak light stimulus ($I_0 \times 2^{-17}$ and $I_0 \times 2^{-16}$) (Fig. 3) evokes single photon responses, bumps. The number of bumps increases with stimulus intensity. Two successive registrations of responses to the β flash ($I_0 \times 2^{-16}$) demonstrate the variability of the responses in the bump range: identical stimuli cause in one case 2, in the other case 5 bumps. With stronger stimulus energies the bumps overlap and fuse to the macroscopic receptor current. Response amplitude and area increase with rising intensity, the time course changes: latency and time-to-peak diminish.

Light adaptation reduces the size of the receptor current. An α response becomes detectable at higher intensities, the amplitude is very small and the latency is shortened compared to the β responses; single bumps are not identifiable. The latency distribution of light-adapted bumps is much narrower than that of dark-adapted bumps [8]; therefore we believe that in

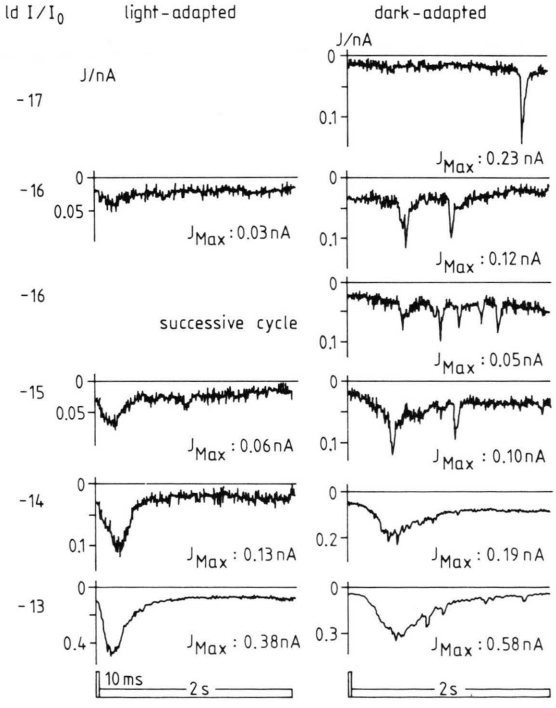

Fig. 3. Receptor currents of *Limulus* ventral nerve photoreceptor recorded in a state of moderate light adaptation (α) and considerable dark adaptation (β) at different flash intensities (ld I/I_0). Intensity of 2 s illumination equivalent to 3.4×10^{14} phot/cm^2, maximal energy of 10 ms α and β flashes equivalent to 9×10^{14} phot/cm^2. 15 °C. Exp. BS8.

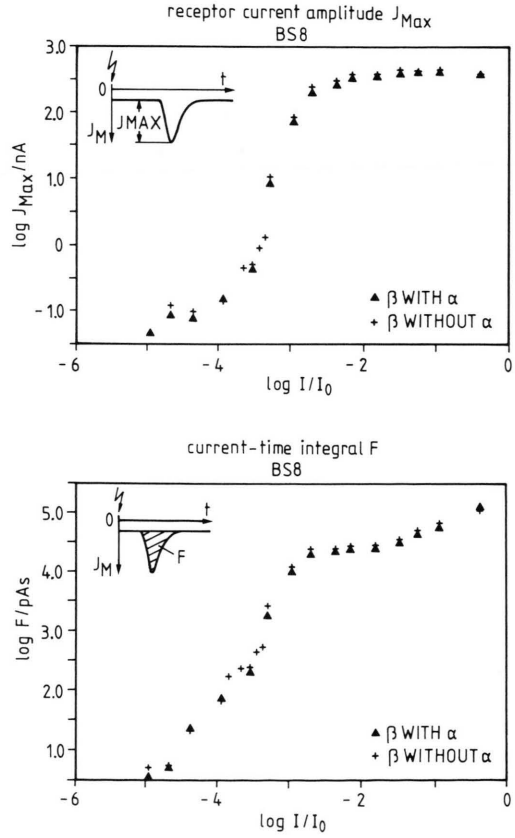

Fig. 4. Response *vs.* energy characteristics of the current amplitude J_{Max} (Fig. 4a) and current-time integral F (Fig. 4b) of β responses with and without preceding α test flash. Intensity of 2 s illumination for both measurements equivalent to 3.4 phot/cm^2, maximal energy of both 10 ms β flashes equivalent to 9×10^{14} phot/cm^2. Exp. BS8.

the light-adapted cell we find directly a complete overlap of the individual bumps. In addition the narrower latency distribution is one reason for the shortening of the response duration.

Influence of the α response on the β response

It is essential for our measurements that the state of adaptation when the β response is evoked is independent from the foregoing α response. In order to test a possible influence of the α response on the size of the β response, we first stimulated the cell with the whole series of light energies for α and β flash and then repeated the same stimulus program with the same cell but omitting the α flash.

Fig. 4 demonstrates the result: J_{Max} and F response *vs.* energy characteristics of β responses with and without preceding α illumination do not differ from each other, *i.e.* the α response does not influence the β response to a significant degree (more details see Table I).

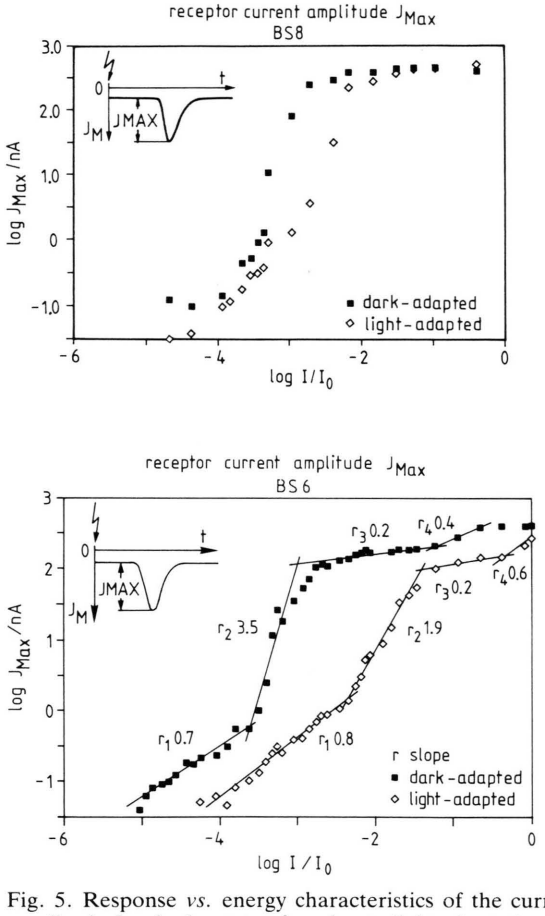

Fig. 5. Response *vs.* energy characteristics of the current amplitude J_{Max} in the state of moderate light adaptation (α) and considerable dark adaptation (β), two different experiments BS8 (Fig. 5a) and BS6 (Fig. 5b). Steepness of sections is determined by linear regression (transient range between section 2 and 3 was not involved in calculation). Intensity of 2s illumination equivalent to 3.4×10^{14} phot/cm^2 (BS8) and 6.7×10^{14} phot/cm^2 (BS6), maximal energy of 10 ms α and β flashes equivalent to 9×10^{14} phot/cm^2. 15 °C.

Response vs. energy characteristics of the current amplitude J_{Max}

In the double logarithmic plot of the amplitude maximum (Fig. 5) of the light-induced receptor current (J_{Max}) versus the light stimulus energy we find different curve sections with different slopes. In the first section s_1 (curve "foot") the slope r_1 [log nA *vs.* log I/I_0] is about 1 (linear section, see Table I), the current amplitude grows in this low energy range, which includes the "bumpy" records (very low energy range), proportional to the light stimulus energy. After the curve "heel" the slope becomes steeper up to the curve "knee" (supralinear "shank" section with a slope r_2 about 3), which characterizes the transition range to a section s_3 with only a slight slope r_3 between 0.1 and 0.2 (thigh, sublinear section). In four of five experiments the response maximum saturates at high light energies; in one experiment, however, we found a second sublinear section (s_4, slope r_4 about 0.5), before the receptor current amplitude seems to reach a saturation level.

To characterize the curve quantitatively we determined steepness, position and extent of the different sections in the log/log plots by linear regression (Fig. 5b).

Response vs. energy characteristics of the dark adapted photoreceptor cell

In the dark-adapted state recognizable bumps (amplitude about 0.05 nA) appear in the energy range of log $I/I_0 \approx -5$ ($I_0\times2^{-16}$ and $I_0\times2^{-17}$), but they vary greatly in size. So we averaged the response values to 2 or 3 flashes from repeated measuring cycles of same stimulus energy. The great bump variability would require the averaging of much more responses, but since we wanted to determine the response characteristics over a great energy range the limited life time of the cell forbade more measurements.

The averaging of 5 experiments (Table I) results in a slope value r_1 of 1.2 ± 0.17 in the foot section of the J_{Max} *vs.* I curve (dark adapted cell). The shank section s_2 rises with a slope r_2 of 3.2 ± 0.19, s_3 with a r_3 of 0.1 ± 0.03. In one experiment a new increase of the curve follows again with a slope r_4 of 0.4.

Heel (s_1-s_2) and knee (s_2-s_3) positions were determined as the points of intersection of the straight regression lines. The energy coordinate of the curve heel is nearly the same in all experiments (log I/I_0: -3.7 ± 0.11, see Table I), the current amplitude ordinate varies more (log J_{Max}: 0.3 ± 0.08) in the concerned experiments. The energy coordinate of the knee is similar too in different experiments (log I/I_0: -3.1 ± 0.10), also the coordinates of the current amplitude in the knee-point do not differ distinctly from one another (log J_{Max}: 2.3 ± 0.11).

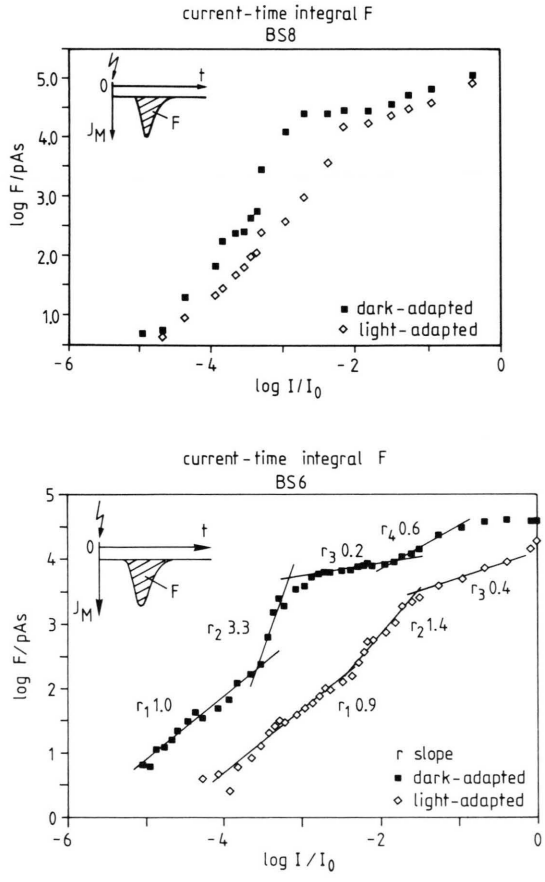

Fig. 6. Response *vs.* energy characteristics of the current-time integral F, same experiments as shown in Fig. 5 (Fig. 6a: BS8, Fig. 6b: BS6). For determination of steepness and transitions of sections see Fig. 5.

Comparison between the response vs. energy characteristics of light- and dark-adapted photoreceptor cells

Transient light adaptation due to the preceding conditioning stimulus reduces the amplitude of the receptor current and shifts the response *vs.* energy characteristics towards higher stimulus energies. The extent of the shifting depends on the conditioning light intensity and on the time of dark adaptation t_{da}.

α and β curves (Fig. 5b) are not exactly parallel: the linear rising foot s_1 of the LA curve has an average steepness r_1 of 1.0 ± 0.07, thus r_1 is slightly smaller in the light-adapted cell than in the dark-adapted one (r_1: 1.2). More pronounced is the difference in section 2: the steepness amounts to 2.8 ± 0.27 for the light-adapted cell compared to 3.2 for the dark-adapted one. Section 3 has a slope of 0.2, which is nearly identical for α and β in this part. Both curves saturate at the same current value.

A comparision between the s_2-s_3 coordinates (knee) of different experiments shows that in the light adapted cell the current amplitudes of the knee are fairly constant, but the corresponding energy values vary clearly. A reason of this fluctuation could be a different rate or time-constant of dark adaptation in different cells.

A comparison between LA α and DA β curves demonstrates a good agreement of the amplitude values in knee position for both states of adaptation:

$$\alpha: 2.4 \pm 0.14 \text{ nA} \quad \beta: 2.3 \pm 0.11 \text{ nA}.$$

The same agreement is found for the heel, which leads to the interpretation that light adaptation shifts the transition points between the characteristic sections to higher light energies, but the amplitude values for the transitions remain about the same, even if the r_2 slopes are different. An explanation could be that some constant cell property, perhaps the area of the microvillus membrane and thereby the number of light-activated ion channels, has an influence on the development of the sections.

Response vs. energy characteristics of the current-time-integral F

The current-time integral (area) F represents a measure of the net charge transported across the cell membrane during a light-induced response and is a relevant parameter for studying the underliying elementary events. Like the current amplitude the current-time integral increases with the stimulus energy in at least 4 clearly recognizable sections of

different slopes (Fig. 6). At low light energies (section 1) the slope r_1 is about 1, in the following supralinear shank section 2 the slope r_2 is greater 2, especially in the dark-adapted cell. A transition range (knee) connects section 2 and 3; 3 has a sublinear steepness. Higher stimulus energies cause a further increase, section 4, which appears to be a prolongation of section 1. In only one out of 5 experiments in the dark-adapted state the responses saturate within the energy range investigated, consequently here we can distinguish 5 sections.

Response vs. energy characteristics of the dark-adapted cell

The smallest bump evaluated has an area about 5 pAs (current 0.05 nA, duration 100 ms).

The largest area measured after illumination with maximal light energy I_0 varied from cell to cell from 40 to 130 nAs.

In the double logarithmic plot the averaged slopes ($n=5$) of the individual sections of the response *vs.* energy characteristics amount to 1.6 ± 0.16 (section 1), 2.7 ± 0.26 (section 2), 0.2 ± 0.03 (section 3) and 0.5 ± 0.12 (section 4), see Table I.

The averaged area coordinates (F values) of the transition points (s_1-s_2 (heel), s_2-s_3 (knee) and s_3-s_4 (hip) vary stronger than the corresponding energy coordinates (for the detailed data see Table I).

Comparison between response characteristics of dark- and light-adapted cells

Light adaptation shifts the response *vs.* energy characteristics towards higher stimulus energies, especially the shifting of the section 2 is clearly recognizable (Fig. 6). In section 1 the α curve (LA) increases less steeply than the dark adapted β curve (α: 1.2 ± 0.09; β: 1.6 ± 0.16). The steepness of section 2 is also lower for LA (r_2: 1.9 ± 0.37) than for DA, but here the scattering of the individual values is greater. In the LA curve it is often difficult to distinguish section 3 (r_3: 0.3 ± 0.07) from section 4.

The characteristic transition points s_1-s_2 (heel) and s_2-s_3 (knee) are found nearly at the same area both for LA and DA:
knee: α: 4.1 ± 0.25 pAs β: 4.1 ± 0.14 pAs
heel: α: 2.1 ± 0.13 pAs β: 2.4 ± 0.13 pAs,
they differ only in the shift of the energy coordinates.

Comparison between current amplitude and current-time integral curves

An essential difference between J_{Max} and F curves consists in the fact that sections 4 can be found in the F graphs of all experiments, but only in one experiment in the J_{Max} graph. (In this experiment, BS6, J_{Max} and F curve (DA) saturate after section 4; the transitions occur at the same light energy for both parameters.) Except for this difference the sensitivity behaviour of both parameters is fairly similar, the effects of light adaptation are nearly the same.

The steepness of the sections s_1, s_2, s_3 is similar for J_{Max} and F curves. The r_1 value of the J_{Max} curve is a little bit smaller than the F r_1. This effect can be caused by the different evaluation methods of the bump values: an increase of the number of single bumps does not cause a great increase in the largest bump amplitude; however the total area is clearly enlarged by the addition. On the other hand J_{Max} (LA and DA) rises steeper in the supralinear section than F (Table I); a reason may be an improvement of bump synchronization with rising stimulus energy, although this bump synchronization should be only small because the difference between the r_2 slope values is only small.

The sublinear r_3 values of the DA curves are almost equal for J_{Max} and F, but a comparison of the LA s_3 sections of J_{Max} and F is difficult because of the inexact definition of s_3 and s_4 in the area curves and the saturation of s_3 in J_{Max} curves (4 of 5 experiments).

Heel and knee of J_{Max} and F curves are at identical energy positions, *i.e.* the individual sections of both parameters correspond to each other, LA and DA transition points differ only in their abscissa value, the ordinate value remains the same for both parameters.

We estimate the number of bumps which constitute the measured macroscopic receptor response for every stimulus energy by extrapolation (assuming linear increase in bump number with increasing light energy) from low stimulus energy, where single bumps can be counted (see Brown and Coles [5]). We can estimate an overlapping of about 30 (the value varies between 15 and 40) bumps in the DA heel and of 100 (the value varies between 75 and 180) bumps in the DA knee.

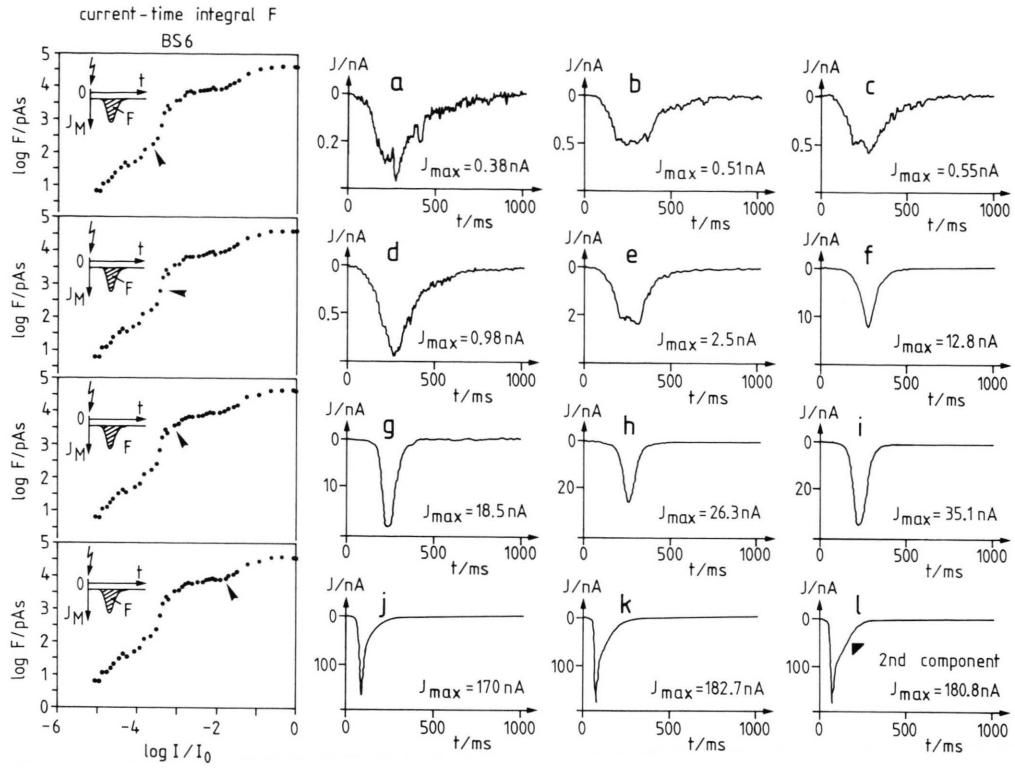

Fig. 7. Receptor currents corresponding to different sections of the response *vs.* energy characteristics of the current-time integral F, Exp. BS6. Record a–l represent responses of the dark adapted photoreceptor cell to test flashes with increasing light energy. The position of the demonstrated responses in the F *vs.* I/I_0 curve is indicated by darts (left column). Record a–c correspond to transition of the linear section s_1 to the sublinear section s_2 of the response *vs.* energy characteristics of the current-time integral, record d–f correspond to s_2, g–i to transition of s_2 to the sublinear section s_3, j–l to transition of s_3 to the second sublinear section s_4.

Receptor current signals at the characteristic transition points heel, knee and hip

Fig. 7 shows responses recorded in characteristic sections of the response *vs.* energy characteristics (area) of the dark-adapted photoreceptor.

In the curve heel region (records a–c) the bumps are not yet completely fused to the smooth macroscopic receptor current. Therefore there is no prominent current amplitude maximum.

Records d–f cover the supralinear range. In this section the amplitude grows by the factor 50, the typical macroscopic response to higher light intensities is formed, the time course is accelerated significantly. In the knee range (records g–i) we find a shortening of the time-to-peak T_{Max}, but the shape of the response does not change further.

The curve hip (records j–m) is characterized by the appearing of the second component of the macroscopic ReC (a second maximum of the receptor current signal, for details see [10], which causes an increase of the response duration and thereby a further increase of the F curve in contrast to the J_{Max} curve.

Attempts to superimpose the response vs. energy characteristics of four different experiments

In order to get a generalized response *vs.* energy characteristic we tried to superimpose the area curves from different cells. Since the curve heel represents a characteristic common point in all experiments, we superimposed the individual curves by shifting in x and y direction to an identical heel position (Fig. 8). The shifting in y direction compensates differences of the current sizes, the shifting in x direction differences of the sensitivities of different cells.

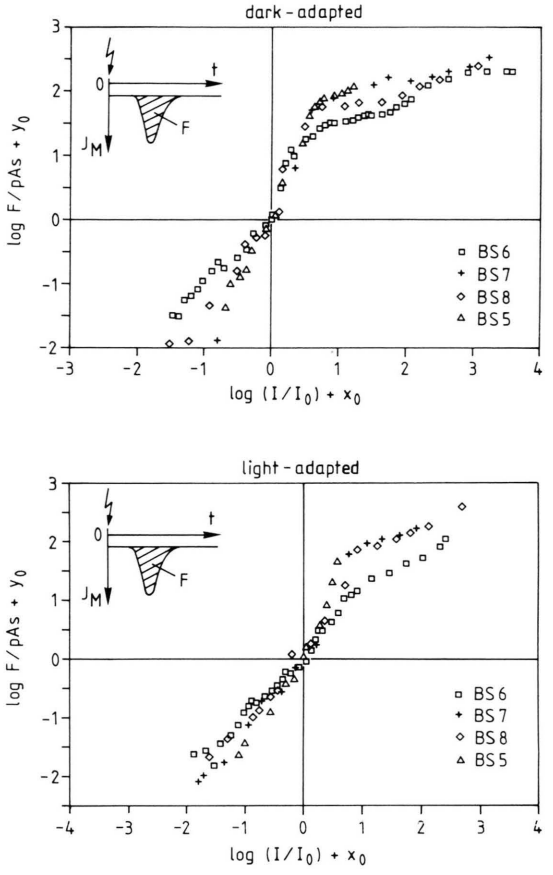

Fig. 8. Response *vs.* energy characteristics of current-time integral F of 4 experiments BS5, BS6, BS7 and BS8 superimposed upon another by shifting of the double-logarithmic plots in x and y direction to identical heel (s_1-s_2, coordinate cross) position determined by linear regression. Fig. 8a: dark-adapted state, Fig. 8b: light-adapted state.

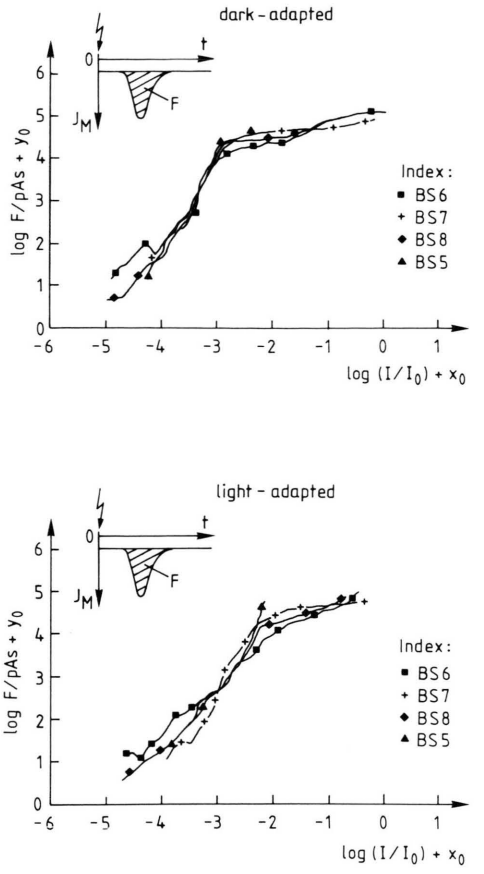

Fig. 9. Response *vs.* energy characteristics of current-time integral F of experiments BS5, BS6, BS7 and BS8 (see Fig. 8) superimposed upon another by shifting the curves in x and y direction to a position with minimal sum of quadratic deviation between y values of compared curves BS5, BS6, BS7 and y values of reference curve BS8. Fig. 9a: dark-adapted state, Fig., 9b: light-adapted state.

The linear sections of the α curves fit well upon one another, although the low energy responses show great variability, but this variability is smaller for LA than for DA. Distinct differences can be seen in the sections s_2 and s_3. In one experiment (BS6) the curve is much less steep compared to the others, the area range of section 2 is smaller and the transition to section 3 occurs at lower ordinate and abscissa values. Therefore the relative area values of section 3 are smaller in this experiment as compared to the other experiments. Different quantum efficiencies and therefore differences in the slopes of the 4 sections can be reasons for the different behaviour of the individual cells. Another explanation is that the knee value represents a characteristic individual cell property and that parameters like cell size or channel density determine the extension of the sections especially of the supralinear section.

Another method to compare different curves is demonstrated in Fig. 9. By shifting of the curves in x and y direction a position was found in which the sum of the quadratic deviation from the y values of the compared curve to a curve used as reference were minimal. The details of this method are described by Betonville [15]. In the case of DA (β) the arrangement of the individual curves to one another is simi-

lar to that of the preceding figure (in which the heel r_1-r_2 was used as coincidence point), *i.e.* in this case both methods lead to the same general result.

The congruence of the LA curves seems to be better when they are projected upon a common heel than by the Betonville-method.

To summarize the results: the response *vs.* energy curves are similar in respect to the deviation into four sections; the heel r_1-r_2 is a characteristic point of this response *vs.* energy dependence, and the slope differences cause at least an important part of the variations between the single experiments.

Time parameters

The time parameters are chosen to characterize the shape *i.e.* the time course of the receptor current signal. All time parameters are shortened by increasing stimulus energy and by light adaptation. Decrease time T_2 and response duration T_B show a complex behaviour. The energy dependence of the following time parameters is described in consideration of the characteristic slope sections s_1, s_2, s_3 and s_4 and the transitions heel and knee of the current amplitude or current area curves.

T_{Lat}: latency

The response latencies to the smallest stimuli correspond to the averaged bump-latency (about 500 ms). In the low energy range which correlates to section 1 (foot) the latency of the dark-adapted cell is reduced about a factor 3 (Fig. 10a). At the beginning of the supralinear section the latency grows with increasing light energy. From the beginning of the curve knee up to section 4 there is again a prominent shortening of T_{Lat}, in section 4 the degree of the shortening becomes smaller. At maximal light energy the latency reaches its shortest value and seems to saturate at 30–40 ms. It is recognizable that the energy dependence of the latency of the β response shows the same partition into the four sections as current amplitude (or area) curves.

In state of light adaptation (α) the energy dependence of T_{Lat} has a much less steep course than in the dark-adapted state, the four sections can be hardly differentiated. At high light energies responses of dark- and light-adapted cells have nearly the same latency.

T_{Max}: Time-to-peak

In the energy regions which correspond to the linear section s_1 and the supralinear section s_2, T_{Max} (time-to-peak) scatters in the described experiment (BS8) around a value of 500 ms (Fig. 10b). This value, which represents the averaged time-to-peak of bumps, varies in different experiments between 300 and 500 ms. Different latency distributions in different cells could be a reason for this variation. With the beginning of the sublinear sections s_3 of the F resp. the J_{Max} curves, T_{Max} is shortened rapidly. The extent of this shortening is greater in s_3 than in the following part s_4. T_{Max} seems to saturate at high light energies below 100 ms.

There is no increase in T_{Max} in section 2 corresponding to the increase in T_{Lat}, although T_{Max} includes the latency. (The latency represents about 70% of T_{Max}.) Perhaps the increase of T_{Lat} here is accompanied with a reduction of the rise time in this section. In LA T_{Max} is 1/3 to nearly 1/2 as great as in DA for s_1 and s_2, but becomes identical for higher energies (s_3 and s_4).

T_1: Half time of increase

The increase time T_1 (Abb. 10c) started with a value about 10 ms at the first detectable bumps and rises to its maximal value (110–170 ms) still in the linear section s_1. The supralinear section s_2 is connected with a strong shortening of T_1. In sections 3 and 4 the decrease is smaller, in two experiments there is a new increase in section 4, but in other experiments T_1 saturates with a value of 10 ms at the beginning of section 4.

The course of the LA T_1 curve is similar to that of the DA T_1 curve, however the T_1 values of sections 1 and 2 are only half as long as in the dark-adapted state and the maximum of the α curve is clearly broader than the maximum of the β curve. At high light energies (s_3 and s_4) the duration of T_1 becomes the same for LA and DA responses, but the LA T_1 becomes longer than the DA T_1 at I_0.

T_2: Half time of decrease

The decrease time T_2 (Fig. 10d) of the receptor current signal shows an energy dependence which has a "N"-shaped course: an increase to a maximum at the beginning, a decrease to a minimum and another increase at the end. The first increase corre-

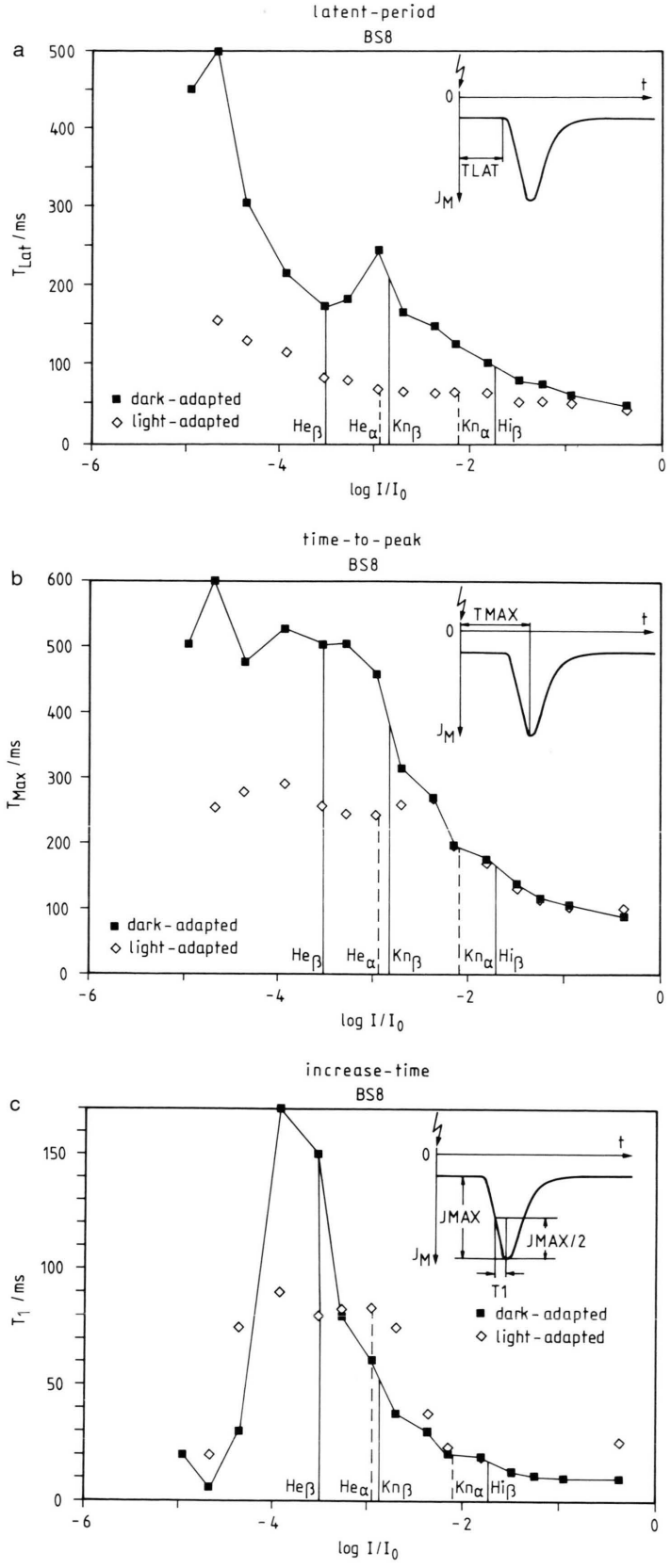

Fig. 10. Time parameter of current responses evoked by test flashes of different light energies in state of considerable dark adaptation (β) and moderate light adaptation (α). Fig. 10a: T_{Lat} (latent-period), Fig. 10b: T_{Max} (time-to-peak), Fig. 10c: T_1 (increase-time), Fig. 10d: T_2 (decrease-time) and Fig. 10e: T_B (duration). He_α and He_β indicate transition s_1-s_2 (heel) in the corresponding α and β response *vs.* energy characteristics of the current-time integral F, Kn_α and Kn_β transition s_2-s_3 (knee), Hi_β transition s_3-s_4 (hip) in dark adapted (β) state. Exp. BS8.

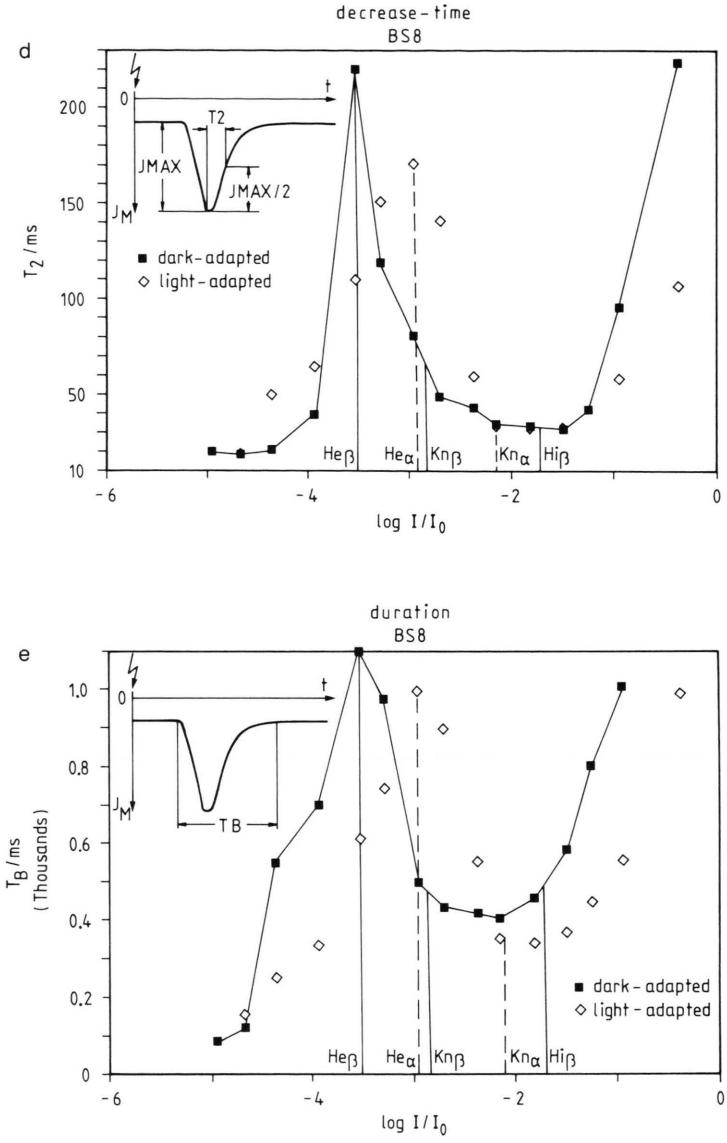

sponds to the linear section s_1, the prominent reduction characterizes s_2 following by section s_3 with only a small reduction of T_2, and the second increase of T_2 occurs in section 4. This second prolongation of the response decline corresponds to the appearance of the second component of the photoreceptor current, see Fig. 7.

In the light-adapted state the T_2-behaviour is similar as in the dark-adapted state, but the curve is shifted by about 0.5 log units to higher energy values.

T_B: Response duration

T_B (Fig. 10d) shows parallel behaviour ("N"-shaped) to T_2. The response decrease is about 2 times longer than the response increase and determines therefore mainly the response duration. T_B increases in section 1 (first increasing "N"-flank) – the response consists of single bumps – up to a T_B of 700–1000 ms. Maximal duration is reached in heel region (see also Fig. 7). In the supralinear section s_2 there is a great shortening (decreasing "N"-flank).

The minimum is reached at the first points of the sublinear section 3. At still higher light energies the response duration increases again (s_4). In 2 of 5 experiments T_B saturates at the highest light energies, in 3 experiments T_B increases up to the last measurement.

In the state of light adaptation we find the same "N"-shaped course shifted by about 1 log unit to higher energies.

The energy dependence of the five time parameters T_{Lat}, T_{Max}, T_1, T_2 and T_B can be divided into four sections with different slope behaviour, the partition is more pronounced in the dark-adapted case than in the light-adapted case. The four sections correspond to the four sections of the J_{Max} and F response *vs.* energy characteristics, the transitions corresponding to heel, knee and hip of the area curve can be found again in the time parameter curves as transition points between the single sections.

Discussion

The response (receptor current) *vs.* stimulus characteristics of the *Limulus* photoreceptor can be subdivided into 4 (current-time integral) or 3 (current amplitude) sections with different slopes:

1) a linear section (slope about 1);
2) a supralinear section (slope about 2–4);
3) a sublinear section (slope < 0.5);
4) a second sublinear section (slope > 0.5).

The macroscopic receptor current consists of a modified sum of overlapping bumps [9]. In the light energy range where individual bumps can be observed the number of bumps increases linearly with the light energy, *i.e.* with the number of absorbed photons [1]. Concerning the different slopes we can say:

Section 1 is consistent with an independent summation of the bumps, in section 2 exists a positive cooperativity between the bumps, they are no longer independent but influence each other with an increasing effect. In sections 3 and 4 the bumps influence each other too, but here with a diminishing effect causing the reduction of the steepness of the response *vs.* energy characteristics.

Two models can explain the observed shape of the response *vs.* stimulus characteristics: the bump-speck model and the model of the attenuation function.

1) Bump-speck model

According to Behbehani and Srebro 1974 and Brown and Coles 1979 [16, 5] absorbtion of a photon causes the opening of light-activated Na^+ channels in a membrane area of 2 μm^2 of the microvillus, in which the photon was absorbed ("bump-speck") [17]. A large bump (1 nA) results from the opening of 1000–2000 channels with a single conductance of about 15 pS [18, 19]. Since the maximal light-induced membrane current is about 1 μA, the total channel number must be about 1 million per cell, that means one channel per microvillus (microvillus number: 1 million [20]). With a microvillus distance of about 100 nm, one can estimate the channel density to *ca.* 100/μm^2 rhabdom [17] and the maximal bump-speck area to about 10 μm^2. (The value may differ from cell to cell.)

If we assume that the ion channels are opened following binding of an internal transmitter and that the binding of more than 1 transmitter molecule *e.g.* 4 (see below) is necessary for the channel opening (Stieve *et al.*, 1986 [7]), and if we further suppose that the transmitter molecules spread from a source by diffusion, we obtain two bump-speck regions: in the central bump-speck region the channels are opened due to the binding of 4 transmitter molecules, but in the surrounding "corona" region the channels are still closed, however "unlocked" due to the binding of 1 or more (but less than are necessary for opening) transmitter molecules [7].

At low light energies there is a formation of isolated bump-specks which are independent of each other, because on the average the membrane areas where photons are absorbed are far away from each other. With increasing light energy the bump-speck density increases, the bump-specks begin to touch and overlap in their "corona" regions. In membrane areas with overlapping "coronas" there might be enough transmitter molecules to open the corresponding channels. This additional charge flow could explain a supralinear curve rise [8]. Further increase of light energy according by further increase of the bump-speck density would cause the touching and overlapping of the central regions of bump-specks; the effective increase of the charge flow would become smaller. Therefore this overlapping of the bump-speck centres can account for a transition to the sublinear section.

According to Brown and Coles 1979 [5] in the dark-

adapted photoreceptor the knee of the response *vs.* energy curves is correlated with a light energy which evokes about 400 bumps during one macroscopic receptor current signal. In their experiments the value varies from 91 to 776. In our experiments the first bumps become detectable at a photon density of 7×10^9 photons/cm^2, the knee can be found at a photon density of 7×10^{11} photons/cm^2. We can calculate that in dark-adapted cells about 100 bumps (± 60) correspond to the knee and about 30 (± 25) to the heel. Therefore the postulated bump-speck centre- and surrounding "corona"-areas are, together, 3–4 times greater than the centre-range alone. If we estimate the bump-speck centre to be about 10 μm^2 (see above) the area of centre and "corona" together must be about 40 μm^2.

Light adaptation shifts the energy coordinates of the knee to higher values. We explain this finding with a reduction of bump-speck size by LA (about a factor which varies between 5 to 20 under our conditions), therefore the more the light adaptation the higher the number of bumps at the knee, an overlapping occurs at higher stimulus energies *e.g.* greater bump-speck density.

The linearity of section 1 (slope 1) applies for current amplitude curves (LA and DA) and for the LA area curves. In DA the averaged value of the area r_1 amounts to 1.5. We have two possibilities to explain this deviation from slope 1:

a) The variety of bumps makes an exact determination of r_1 difficult, and the deviation from slope 1 may depend on a deficiency of measured data. However slope 1 can be expected from the assumption of a linear increase of bump number with increasing light energy. We find slope 1 in experiments with many measured values in the low energy range, slope 1 applies for the α curves and is confirmed in current amplitude measurements from Lisman and Brown 1975 [4].

b) A second explanation would postulate a non-independence of bumps already in this section, for example as a consequence of a small facilitation (see below).

The slope of section 2 amounts to ≥ 3 (3.1 ± 0.37 for the J_L curve and 2.9 ± 0.29 for the F curve) in the state of dark adaptation. Our main intention is to investigate the slope of the area curve, because these values consider the total number of bumps, in contrast to the current amplitude values which represent a measure of the maximal number of simultaneously formed bumps. Supralinear behaviour was found by many authors [5, 9, 21, 22, 23], the slope values vary between 2 and 4. A 2 ligand model allows a maximal slope value of 2. The presented results indicate a cooperativity of at least 4. This value is not quite reached, but the results show a value of 3 and more (β: 2.7–3.5) and since the slope of a log/log plot always represents the minimal number of cooperating ligands, we suggest a cooperativity of 4.

A cooperativity of 4 resp. the binding of 4 transmitter molecules is also supposed in vertebrates [24, 25].

However, a cooperativity of 4 does not necessary mean that 4 transmitter molecules have to be bound to the channel to open it. It could be achieved also if 4 ligands have to be bound at other stages of the transduction chain, or if two consecutive cooperativities of 2 – perhaps the transmitter binding delivers a factor 2 and the additional rise has to be searched for in other parts of the transduction chain – are involved.

The supralinear slope can be caused by a supralinear increase of bump number or, as supposed by Grzywacz and Hillman [26] by an increase of the bump amplitude, or by both effects together, that means the quantum efficiency for bump generation can be changed. A comparable effect, which occurs at lower stimulus energies as supralinearity, is described as facilitation [9, 27]: a very low conditioning flash 2 seconds before the bump-evoking flash causes an increase in size and number of the evoked bumps. Facilitation could also be explained by the same model which requires the binding of more than one transmitter molecule to open the light activated channels.

It must be investigated whether supralinearity is caused by the same phenomenon as facilitation which starts during the response itself. The supralinear slope is not caused by a better synchronization of the bumps [7], because this effect would require a slope greater than 1 only of the current amplitude curve but not as described in our experiments of the area curve. The sublinear section s_3 with a slope smaller than 0.5 can not be explained with the simplest form of the bump-speck model (without further assumptions the model would require a saturation-level at higher light energies); one of those assumptions might be that not all channels are opened in the bump-speck centre, so that a further light energy increase could open additional channels.

We find a saturation after s_3 in some experiments for the current amplitude curves but on no account for the area curves. In case of saturation the same J_{Max} saturation value is reached for light- and dark-adapted cells. Reaching a common saturation value and shifting of the knee position to higher light energies at constant ordinate-values are consequences of the bump-speck model if we assume that light adaptation reduces the bump-speck diameter.

After this sublinear section a new slope increase follows, visible in all area curves and in one current-amplitude curve. Four reasons can explain this effect:

a) A further 30–50% of the channels could be opened.

b) The second explanation considers the increase of the response duration (see Fig. 10e) just at that energy region at which we find the new slope increase of section 4 in the area curves and saturation in the most amplitude curves. A surplus of transmitter molecules at high light energies could cause a repeated opening of ion channels. On this condition the area curve would saturate when there are no more transmitter molecules, the current-amplitude curve would saturate when all channels are open.

c) Another possibility to explain the two sublinear slopes is to assume that the channels could have two different conducting states (as suggested by Bacigalupo and Lisman 1983 [19] and Nagy, unpublished).

d) Different types of ion-channels with different conducting properties could be responsible for different slope sections.

2) Automatic gain control

Additional to the bump-speck-model another model has to be considered: this model is based on the conception that the first bumps appearing during a response influence the following in an adapting manner, so that the latest bumps after a light stimulus are the most suppressed. This feed-back mechanism diminishes later occurring response parts and can explain that the time course of the macroscopic receptor current is much faster than that of an independent artificial bump sum. We can describe this effect with the attenuation function a(t) [7, 28]. The method allows us to simulate an energy dependence of the photoreceptor current, which shows two slope sections: a linear slope section up to a curve bend (knee) and a sublinear section at higher light energies. The steepness of the sublinear section is determined by the strength of feed-back *i.e.* by the value of a(t). A simple feed-back mechanism would reduce the slope maximally to 0.5. Perhaps some other factor, which limitates or stops the effectivity of the attenuation function, could be the reason for a third section. Besides the two slope sections the convolution of the bump-sum with the a(t) function simulates the two components of the current response (see above), the appearance of which depends on light energy and adaptation level [7], and also imitates adapting effects.

The automatic gain involved here contains no explanation of the supralinearity, which has to be provided by an additional *e.g.* bump-speck mechanism.

Light adaptation

Light adaptation shifts the sensitivity curve to higher energies. The adaptation depends markedly upon the external calcium concentration [7]. According to the adapting bump model light adaptation reduces the bump size by diminishing the amplification degree between absorbed photon and the opening of ion-channels. Smaller bumps mean smaller bump-specks, which can explain the shifting of heel and knee towards higher intensities, but not the reduced supralinearity in s_2 for the LA cells, because the decrease of the bump-speck diameter without further assumptions should not have any effect on the slopes. Possibly adaptation could also influence the cooperativity and by this the slope.

Time parameters

The time parameters of the receptor current signal are determined by the distribution of the bump latencies and the time-dependent (after stimulus) attenuation of the bump sizes (a(t) function). The energy dependence shows a reduction of the time parameters, especially in the energy range, which corresponds to the supralinear section of the J_L and F curves (except for latency and time-to-peak). With increasing light energy the probability increases that bumps with very short latencies occur. Since the latency of the receptor current response is determined by the shortest bump latency, it should be clear that higher light energies shorten the macroscopic response latency. We can not explain the finding of a

latency increase in the supralinear section by this simple concept.

The increase of the parameters T_2 and T_B with high light energy (s_4) could be a consequence of an exhaustion of the attenuator, or an indication of a repeated opening of the ion channels or of an involvement of other channels with different conductance (see above).

Light adaptation narrows the bump latency distribution and shifts its maximum towards smaller values, an effect which is observed at least for the low energy range where individual bumps can be observed [8] and supposed to be the reason why the α time parameters are smaller and their characteristical sections shifted to higher light energies.

To summarize the results we can say that we find four sections with different slopes in the response *vs.* energy characteristics. We explain the different slopes with different rates of cooperativity.

The energy dependence of the time parameters shows the same partition in 4 sections as the receptor current. Light adaptation shifts the response *vs.* energy characteristics towards higher stimulus energies. Light adaptation reduces also the time parameters.

Bump-speck-model and attenuation function together give sufficient explain for most of the observed phenomena.

Acknowledgements

We thank T. Hennig for technical help, H. Gaube, H. Reuss, M. Naynert for critical reading of the manuscript.

[1] S. Yeandle and M. G. F. Fuortes, J. Physiol. **47,** 443–463 (1964).
[2] J. Scholes, Cold Spring Harbour, Symp. Quant. Biol. **30,** 517–527 (1965).
[3] F. A. Dodge, B. W. Knight, and J. I. Toyoda, Science **160,** 88–90 (1968).
[4] J. E. Lisman and J. E. Brown, J. Gen. Physiol. **66,** 473–488 (1975a).
[5] J. E. Brown and J. A. Coles, J. Physiol. **296,** 373–392 (1979).
[6] H. Stieve and M. Pflaum, Vis. Res. **18,** 747–749 (1978).
[7] H. Stieve, H. Gaube, and J. Klomfaß, Z. Naturforsch. **41c,** 1092–1110 (1986).
[8] H. Stieve, in: Molecular mechanism of photoreception (H. Stieve, ed.), Dahlem Konferenzen, pp. 199–230, Springer Verlag, Berlin, Heidelberg, New York, Tokyo 1986.
[9] H. Stieve, M. Bruns, and H. Gaube, Z. Naturforsch. **38c,** 1043–1054 (1983).
[10] I. Claßen-Linke and H. Stieve, Z. Naturforsch. **41c,** 657–667 (1986).
[11] H. Stieve and M. Bruns, Z. Naturforsch. **33c,** 574–579 (1978).
[12] H. Stieve, M. Pflaum, J. Klomfaß, and H. Gaube, Z. Naturforsch. **40c,** 278–295 (1985).
[13] H. Stieve, M. Bruns, and H. Gaube, Z. Naturforsch. **39c,** 662–679 (1984).
[14] I. Claßen-Linke and H. Stieve, Biophys. Struct. Mech. **7,** 336–337 (1971).
[15] J. Betonville, Diplomarbeit, RWTH Aachen, F.R. Germany, 1986.
[16] M. Behbehani and R. Srebro, J. Gen. Physiol. **64,** 186–200 (1974).
[17] W. Keiper, J. Schnakenberg, and H. Stieve, Z. Naturforsch. **39c,** 781–790 (1984).
[18] F. Wong, B. W. Knight, and F. A. Dodge, J. Gen. Physiol. **76,** 517–537 (1980).
[19] J. Bacigalupo and J. E. Lisman, Nature **304,** 268–270 (1983).
[20] J. E. Lisman and H. Behring, J. Gen. Physiol. **70,** 621–633 (1977).
[21] J. A. Coles and J. E. Brown, Biochim. Biophys. Acta **436,** 140–153 (1976).
[22] A. Fein and J. S. Charlton, J. Gen. Physiol. **69,** 553–569 (1977).
[23] N. M. Gryzwacs, Thesis, Hebrew University, Jerusalem 1984.
[24] L. W. Haynes, A. R. Kay, and K. W. Yau, Nature **321,** 66–70 (1986).
[25] N. J. Cook, W. Hanke, and U. B. Kaupp, Proc. Natl. Acad. Sci. U.S.A. **84,** 585–589 (1987).
[26] N. M. Gryzwacz and P. Hillman, Proc. Natl. Acad. Sci. U.S.A. **82,** 232–235 (1985).
[27] H. Stieve and M. Bruns, Biophys. Struct. Mech. **6,** 271–285 (1980).
[28] H. Stieve, J. Schnakenberg, A. Kuhn, and H. Reuss, Fortschritte der Zoologie **33** (1986).